# Evaluation of Fractional Slot Concentrated Winding Permanent Magnet Synchronous Machine for Electric Vehicle Application


Anqing He
Zhejiang CRRC electric vehicle Co.Ltd
Ningbo, China
hunter1800@163.com

Chenxi Zhou
College of Electrical engineering
Zhejiang University
Hangzhou, China
21610044@zju.edu.cn

Xiaoyan Huang
College of Electrical engineering
Zhejiang University
Hangzhou, China
xiaoyanhuang@zju.edu.cn

Jianxin Shen
College of Electrical engineering
Zhejiang University
Hangzhou, China
J_X_Shen@zju.edu.cn

Youtong Fang
College of Electrical engineering
Zhejiang University
Hangzhou, China
youtong@zju.edu.cn

Qinfen Lu
College of Electrical engineering
Zhejiang University
Hangzhou, China
luqinfen@zju.edu.cn



***Abstract*—This paper mainly designed and compared the fractional slot concentrated winding (FSCW) permanent magnet synchronous motors (PMSMs) with different rotor topologies. To obtain higher peak torque with the constrain for cogging torque and torque ripple, three kinds of motors with different rotor topologies, including surface-mounted rotor, rectangular interior rotor and V-type interior rotor, are optimized using Maxwell. The optimized motors are further analyzed and compared with their electromagnetic performance at no load and its efficiency map. It turns out that higher peak torque can be achieved with surface-mounted rotor topology while V-type interior rotor has better performance in terms of efficiency map.**



***Keywords—Fractional slot concentrated winding (FSCW), different rotor topologies, torque optimization, performance comparison.***


## I. INTRODUCTION

Fractional slot concentrated winding (FSCW) permanent magnet synchronous motor (PMSM) is welcomed and widely used in many applications for its advantages of short winding ends, low cogging torque, high torque density, high efficiency and good flux-weakening capability [1]. There are many researches on FSCW permanent magnet synchronous motors in different aspects, including the torque ripple, vibration and noise, pole-slot combination, constant power speed region operation and efficiency [2]-[5]. It is found out that the torque ripple is independent of cogging torque in terms of salient pole machines [2]. The comparison between FSCW machines and integer slot distributed winding (ISDW) machines has also been researched a lot [6]. However, there still remains a lot of work to do when considering about the motor performances of FSCW PMSM with different rotor topologies, which is also an important issue for electric vehicle application.

This paper mainly designed and compared the 10-pole-12-slot permanent magnet synchronous motors with three different rotor structures, named as surface-mounted permanent magnet synchronous motor (SPM), rectangular interior permanent magnet synchronous motor (RIPM), and V-type interior permanent magnet synchronous motor (VIPM), respectively. In section II, three motors are designed and optimized to achieve higher peak torque with the constrain for torque ripple and cogging torque with the same motor main dimension. With the optimized motors, more information of the motors including electromagnetic performance at no load and the efficiency map are simulated and further compared in section III.

## II. MODEL DESIGN AND TORQUE OPTIMIZATION

### A. Motor Structures

To compare the three motors with different rotor topologies, basic restrictions are defined to obtain appropriate comparison results considering practical applications in electrical vehicles. The constrains are as follows: outer diameter $D_{o1}$=236 mm, stack length $L_{ef}$=100 mm, air gap length g=0.8 mm, shaft diameter $D_{i2}$=60 mm, slot fill factor $S_f$=0.55, current density J=19.58 $A_{rms}/mm^2$ and the same amount of permanent magnet. Besides, the slot-pole combination is chosen as 10-pole-12slot for its high fundamental winding coefficient and low cogging torque. Furthermore, the DC bus is fixed at 374 V and the basic speed is at 3070 rpm, which indicts the same number of conductors per slot. The structures of the three motors with parameters to be optimized are demonstrated in Fig. 1. It is deserved to be mentioned that rib1 and rib3 are important parameters that influence the flux leakage of the permanent magnet and thus the peak torque. Therefore, rib1 is set as 1 mm in this paper for VIPM and RIPM for better comparison and rib3 equals 2 mm.

### B. Torque Performance Optimization

Motors with proposed parameters in Fig. 1 are optimized using Maxwell with finite element method (FEM).

For stator part, it is optimized with the method proposed in [4] and it turns out that the peak torque can be achieved when the split ratio is equal to 0.68 and the teeth width and the slot width share the same length for all three motors. For different motors, the optimal stator parameters are similar,


This work was supported by the National Natural Science Foundation of China (51877196), Key R&D Program of Zhejiang(2019C01075), Ningbo Innovation 2020 program and the Cao Guangbiao High Tech Development Fund of Zhejiang University.

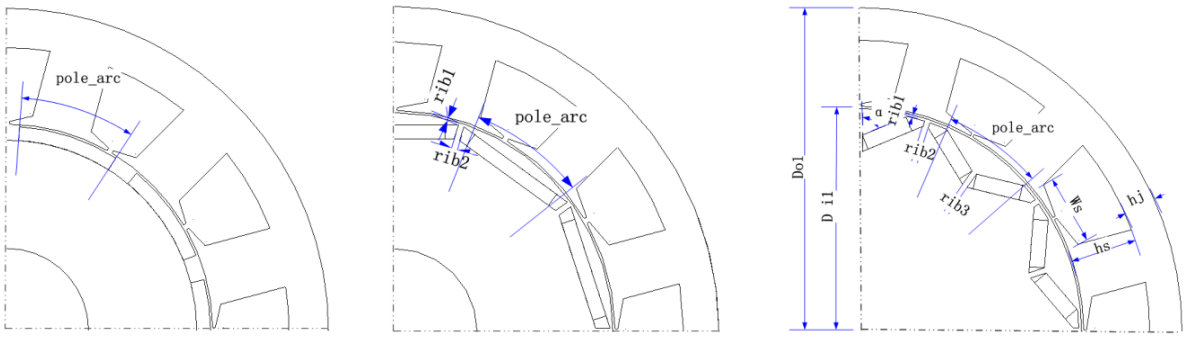


(a) (b) (c)

Fig. 1. Motor structures with respective optimization parameters. (a). SPM. (b). RIPM. (c).VIPM. ($D_{o1}$:the outer diameter of the motor, $D_{i1}$=$D_{o1}$*ratio_D: the inner diameter of the motor, Ratio_D: split ratio, $h_j$: stator yoke height, $h_s$: height of the slot, $w_s$: width of the slot, pole-arc: pole-arc coefficient of the magnet. rib1: the distance between the magnet bridge outer edge and the rotor outer edge for RIPM and VIPM, rib2: the distance between the adjacent permanent magnet bridge for RIPM and VIPM, rib3: the distance between magnet bridge in one V-shape permanent magnet for VIPM and α: the magnet field angle for VIPM.)

meaning that the stator structure have no much impact on motors with different rotor structures. Thus, the stator structure is designed identical for different motors.

With the settled stator dimension, the position of the permanent magnet in rotor is further optimized. For different motors, pole-arc matters most and its relationship between the peak torque, torque ripple and cogging torque for the three motors are shown in Fig. 2. For VIPM, the magnet field angle α and the pole-arc of the motor are optimized together for their correlation. Other parameters relevant with magnet bridge for IPMs are further simulated and the results are depicted in Fig. 3.

From Fig. 2(a)-(c), it can be concluded that the relationship between the cogging torque and the pole-arc is not monotonous and the optimal pole-arc for different motors varies. For VIPM, the optimal pole-arc for lowest cogging torque increases with the larger α, ranging from 0.76 to 0.78. However, the lowest cogging torque for different α of VIPM is almost the same at the respective optimal pole-arc. Moreover, the cogging torque of RIPM is lower than the other two on the whole and SPM has worst performance in terms of cogging torque. As for the peak torque and the torque ripple shown in Fig. 2(d)-(f), all of the three motors have higher torque applied with bigger pole-arc, while the torque ripple curve for SPM and IPMs is quite different.. It is hard to get both high peak torque and low torque ripple with the same pole-arc for IPMs, but easy to be achieved for SPM. In addition, the smaller α is a better choice for higher peak torque while causing the larger torque ripple at the same time. In order to get the cogging torque lower than 3 Nm and the torque ripple lower than 6.5%, the pole-arc for SPM is chosen at 0.79 and 0.68 for RIPM and VIPM. The magnet field angle α for VIPM is chosen at 135 deg.

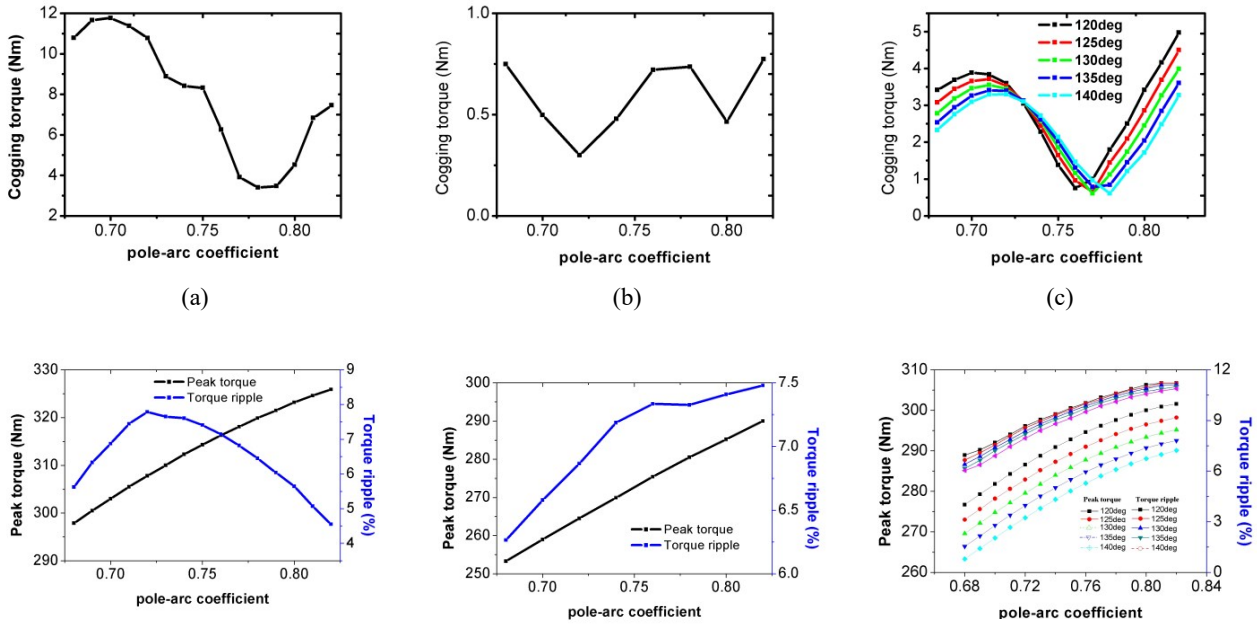


(a) (b) (c)

(d) (e) (f)

Fig. 2. Motor: cogging torque, peak torque and torque ripple varied with pole-arc (and α for VIPM) . (a). SPM. (b). RIPM. (c). VIPM. (d). SPM. (e). RIPM. (f). VIPM

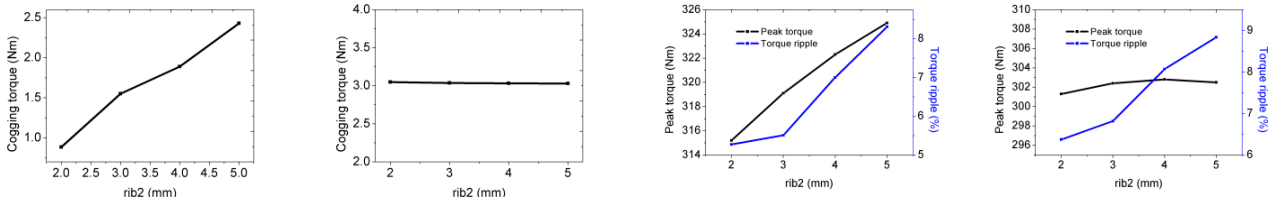


Fig. 3. Cogging torque, peak torque and torque ripple varied with rib2. (a). RIPM. (b). VIPM. (c). RIPM. (d). VIPM.

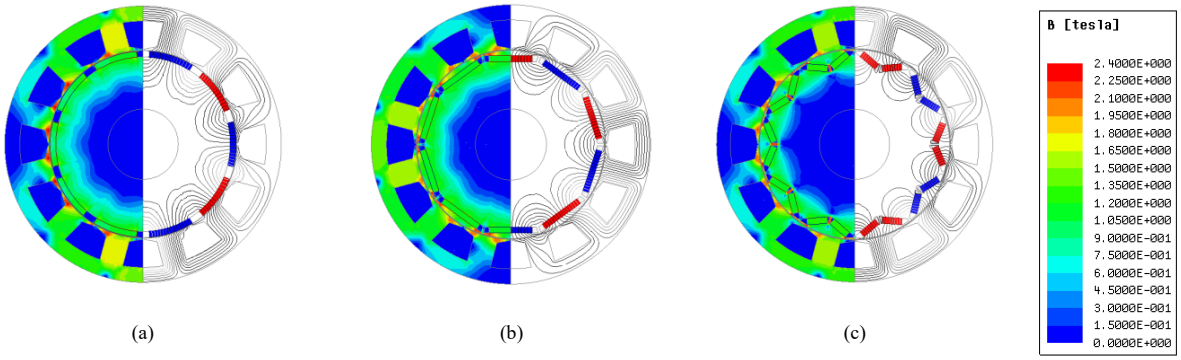


Fig. 4. Flux density distribution at no load: (a). SPM.(b). RIPM. (c). VIPM.

From Fig. 3, the influences of rib2 on different kinds of motors are not the same. For VIPM, rib2 has great impact on the torque ripple, but little effect on cogging torque and peak torque. With the larger rib2, the position of the V-type permanent magnet is not changed but the gap between the adjacent magnet bridge is bigger. It leads to the change in the magnetic flux density waveform in the air gap, causing higher torque ripple. The relation between rib2 and torque ripple in RIPM is similar with VIPM. For RIPM, with larger rib2, the permanent magnet in RIPM is closer to the stator and the usage of the permanent magnet increases a little, leading to the higher peak torque.

TABLE I. MOTOR DESIGN

| Parameters | Motor Type | | |
|---|---|---|---|
| | ***SPM*** | ***RIPM*** | ***VIPM*** |
| Stator dimension | | | |
| Ratio_D | 0.68 | | |
| $w_s$ (mm) | 23.68 | | |
| $h_s$ (mm) | 23.19 | | |
| $h_j$ (mm) | 13.56 | | |
| Rotor dimension | | | |
| Pole_arc | 0.79 | 0.68 | 0.68 |
| $m_{PM}$ (kg) | 1.137 | | |
| Rib1 (mm) | / | 1 | 1 |
| Rib2 (mm) | / | 2 | 2 |
| Rib3 (mm) | / | / | 2 |
| α | / | / | 135 |
| | | | |
| Cogging torque (Peak to Peak) (Nm) | 2.75 | 0.86 | 2.45 |
| Peak Torque (Nm) | 295 | 247 | 259 |
| Torque ripple (%) | 5.16 | 6.48 | 6.50 |

With the constraints mentioned in Section II. A and the parameters optimized above, the final design results of the motors are listed in TABLE I. The mechanical stress of the three motors are also verified in order to operate at the maximum speed, 12000 rpm. As shown in TABLE I, SPM has higher peak torque and lower torque ripple than IPMs while the cogging torque is the highest. As for IPMs, VIPM has slight advantage over the RIPM in terms of peak torque owing to its ability of gathering magnetic field. More motor performances are further simulated and compared in Section III to get a deeper understanding for the three motors.

## III. PERFORMANCE COMPARISON

### *A. Electromagnetic performance at no load*

For the optimized motors, their electromagnetic performances at no load are analyzed and compared. Fig. 4 shows the flux density distribution of the three motors. It can be seen that all three motors have high magnetic flux density around the teeth tip and flux line goes directly from the S-pole permanent magnet to the teeth and straight back to the N-pole permanent magnet, which induced flux leakage and contributed to the higher inductances of the motor. For RIPM and VIPM, there are extra flux leakage around the magnet bridge, which lead to the even lower main flux linkage and lower line-line voltage as a consequence. It can be observed in Fig. 5 that SPM has the highest line-line voltage and RIPM is the lowest, which is coincident with the results of the peak torque of the motors. RIPM has the least total harmonic distortion (THD) of the voltage and the lowest cogging torque as a result. For SPM and VIPM, the $11^{th}$ and $13^{th}$ harmonic predominate in all kind of harmonics.

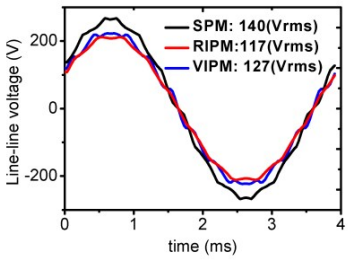


(a)

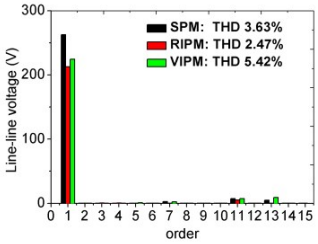


(b)

Fig. 5. (a).Line-line voltage waveforms. (b). Fourier decomposition.

### B. *Efficiency map*

Furthermore, the efficiency map is simulated and demonstrated in Fig. 6. The losses, including copper loss, iron loss, magnet eddy current loss and mechanical loss is considered and simulated. The mechanical loss is set as 400 W at 3070 rpm. For different motors, the stator part is identical, meaning the same winding resistance and current supply. As a consequence, the copper loss of the three motors are similar. The iron loss and the magnet eddy current loss is quite different owing to the different magnetic density distribution.

As shown in Fig. 6, the efficiency of VIPM is higher than SPM and RIPM on the whole. VIPM has wider high efficiency range (efficiency higher than 95%) in the low speed range and obviously higher efficiency in high speed range than SPM and RIPM. In the low speed region, copper loss predominates, which resulted in the similar efficiency performance. However, with either higher current or larger speed, the iron loss and the magnet eddy current loss become larger. Compared to SPM, IPMs have lower magnetic density, resulting in lower iron loss and magnet eddy current loss. Therefore, the efficiency of IPMs are higher in the high speed region and high current region. For IPMs, VIPM has even better efficiency performance owing to its separated permanent magnets. The separated permanent magnets is an effective way to block the permanent magnet eddy current path, which is good for the reduce of the magnet eddy current loss.

## IV. Conclusion

This paper aims to compare the torque performances and the efficiency of three motors with different kinds of rotor topologies. It is optimized with constraints including motor dimensions, the same stator part and the permanent magnet usage to achieve high torque with relatively low cogging torque and torque ripple. SPM has high peak torque for its less flux leakage, compared to IPMs. Furthermore, VIPM is a little better than RIPM in terms of torque performance owing to its assembled magnetic. In addition, lower torque ripple can be achieved by SPM while IPMs are preferred if lower cogging torque is required.

Their electromagnetic performance at no load and the efficiency map are further analyzed to get deeper comparison for the motors. For SPM, there is less flux leakage and higher magnetic density, causing the higher iron loss and magnet eddy current loss. Hence, the efficiency of SPM is lower than IPMs, especially in the high current region and high speed region. Due to the separated permanent magnets, the magnet eddy current loss is even lower for VIPM, and thus the better efficiency performance.

As a consequence, it is a compromise to achieve the high peak torque and high efficiency when choosing the appropriate rotor topology.

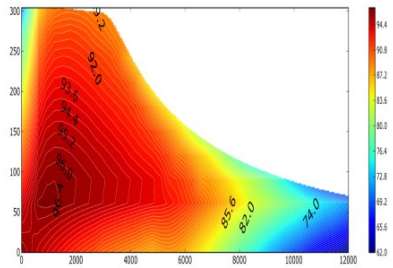

(a)

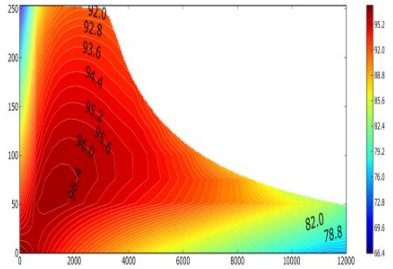

(b)

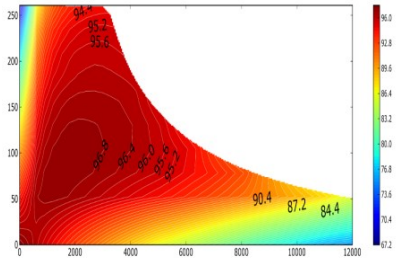

(c)

Fig. 6. Efficiency map: (a). SPM.(b). RIPM. (c). VIPM.

## References

[1] A. M. EL-Refaie, "Fractional-Slot Concentrated-Windings Synchronous Permanent Magnet Machines: Opportunities and Challenges," in IEEE Transactions on Industrial Electronics, vol. 57, no. 1, pp. 107-121, Jan. 2010.

[2] S. Yang, B. C. Mecrow, N. J. Baker, C. Hilton, D. K. Perovic and I. Kakavas, "Torque ripple reduction in fractional-slot concentrated-winding machines with saliency," 8th IET International Conference on Power Electronics, Machines and Drives (PEMD 2016), Glasgow, 2016, pp. 1-5.

[3] Y. Kai, Y. Jianhu, Z. Shangkun, W. Pan and F. Yi, "Study on vibration and noise of fractional slot IPMSM for electric vehicle based on multi-physical field coupling method," IECON 2017 - 43rd Annual Conference of the IEEE Industrial Electronics Society, Beijing, 2017, pp. 2196-2200.

[4] E. Carraro, N. Bianchi, S. Zhang and M. Koch, "Design and Performance Comparison of Fractional Slot Concentrated Winding Spoke Type Synchronous Motors With Different Slot-Pole Combinations," in IEEE Transactions on Industry Applications, vol. 54, no. 3, pp. 2276-2284, May-June 2018.

[5] J. Mun, G. Park, S. Seo, D. kim, Y. Kim and S. Jung, "Design Characteristics of IPMSM With Wide Constant Power Speed Range for EV Traction," in IEEE Transactions on Magnetics, vol. 53, no. 6, pp. 1-4, June 2017, Art no. 8105104.

[6] A. Wang, C. Wang and W. L. Soong, "Design and optimization of interior PM machines with distributed and fractional-slot concentrated-windings for hybrid electric vehicles," 2014 IEEE Conference and Expo Transportation Electrification Asia-Pacific (ITEC Asia-Pacific), Beijing, 2014, pp. 1-5.